Experimental Animals
Exp. Anim. 73(4), 376–389, 2024

Original

Ectodysplasin-A2 receptor (EDA2R) knockdown alleviates myocardial ischemia/reperfusion injury through inhibiting the activation of the NF-κB signaling pathway

Zhi-Hui GUAN[1)], Di YANG[2)], Yi WANG[1)], Jia-Bin MA[3)] and Guo-Nian WANG[1)]

[1)]*Department of Anesthesiology, the Fourth Affiliated Hospital of Harbin Medical University, No. 37, Yiyuan Street, Harbin, 150001, P.R. China*
[2)]*Department of Anesthesiology, Heilongjiang Hospital, Beijing Children's Hospital, Capital Medical University, No. 57, Youyi Road, Harbin, 150028, P.R. China*
[3)]*Department of Medical Service, Heilongjiang Province Healthcare Security Administration, No. 68, Zhongshan Road, Harbin, 150036, P.R. China*

Abstract: Ischemia/reperfusion (I/R) is a pathological process that occurs in numerous organs and is often associated with severe cellular damage and death. Ectodysplasin-A2 receptor (EDA2R) is a member of the TNF receptor family that has anti-inflammatory and antioxidant effects. However, to the best of our knowledge, its role in the progression of myocardial I/R injury remains unclear. The present study aimed to investigate the role of EDA2R during myocardial I/R injury and the molecular mechanisms involved. *In vitro*, dexmedetomidine (DEX) exhibited a protective effect on hypoxia/reoxygenation (H/R)-induced cardiomyocyte injury and downregulated EDA2R expression. Subsequently, EDA2R silencing enhanced cell viability and reduced the apoptosis of cardiomyocytes. Furthermore, knockdown of EDA2R led to an elevated mitochondrial membrane potential (MMP), repressed the release of Cytochrome C and upregulated Bcl-2 expression. EDA2R knockdown also resulted in downregulated expression of Bax, and decreased activity of Caspase-3 and Caspase-9 in cardiomyocytes, reversing the effects of H/R on mitochondria-mediated apoptosis. In addition, knockdown of EDA2R suppressed H/R-induced oxidative stress. Mechanistically, EDA2R knockdown inactivated the NF-κB signaling pathway. Additionally, downregulation of EDA2R weakened myocardial I/R injury in mice, as reflected by improved left ventricular function and reduced infarct size, as well as suppressed apoptosis and oxidative stress. Additionally, EDA2R knockdown repressed the activation of NF-κB signal *in vivo*. Collectively, knockdown of EDA2R exerted anti-apoptotic and antioxidant effects against I/R injury *in vivo* and *in vitro* by suppressing the NF-κB signaling pathway.
Key words: apoptosis, dexmedetomidine, ectodysplasin-A2 receptor (EDA2R), myocardial ischemia/reperfusion, NF-κB

Introduction

Ischemic heart disease is one of the leading causes of death worldwide [1]. Myocardial ischemia/reperfusion (I/R) injury is the main cause of mortality and morbidity in patients with ischemic heart disease [2]. I/R results in the destruction of the myocardial cellular structure and the disturbance of myocardial cell energy metabolism, thus leading to myocardial tissue infarction [3]. Notably, I/R injury often contributes to increased oxidative stress, thus triggering cell apoptosis [4]. Inhibition of oxidative stress and apoptosis has therapeutic significance for I/R injury [5]. Therefore, it is essential to explore the molecular mechanisms of oxidative stress

(Received 25 February 2024 / Accepted 21 May 2024 / Published online in J-STAGE 25 May 2024)
Corresponding author: G.-N. Wang. email: wang66laoshi@126.com

and apoptosis during myocardial I/R injury to develop effective therapeutic strategies.

Ectodysplasin-A2 (EDA-A2) receptor (EDA2R), also known as X-linked ectodermal dysplasia receptor, is a recently isolated member of the TNF superfamily. Increasing evidence has suggested that EDA2R promotes apoptosis in multiple types of cells [6–9]. EDA-A2 induces Dickkopf-1 (DKK-1) secretion and causes apoptosis in human hair follicle (HF) cells by binding EDA2R [10]. Lan *et al*. corroborated that EDA2R induced podocyte apoptosis and dedifferentiation under high-glucose conditions [11]. Furthermore, knockdown of EDA2R reduces cell apoptosis, and exerts anti-inflammatory and antioxidant effects against hyperoxia-induced injury in lung epithelial cells [12]. These reports indicated that EDA2R may be involved in regulating cell apoptosis and oxidative stress. Data from the Gene Expression Omnibus (GEO) database (GSE160516) demonstrated that EDA2R expression was elevated in the myocardial tissues of a mouse myocardial I/R model. However, the role of EDA2R in myocardial I/R injury remains poorly understood.

Under resting conditions, inactive NF-κB dimers (classically p65/p50) bind to IκB in the cytoplasm. While stimulated, IκB kinase mediated-IκB phosphorylation results in IκB ubiquitination and nuclear translocation of NF-κB [13, 14]. NF-κB signaling regulates the expression of genes that coordinate stress, growth and inflammatory responses [15]. NF-κB signal is activated by oxidative stress and its activation can be modulated by antioxidant compounds [16]. Inhibition of NF-κB has been shown to induce apoptosis in multiple types of cells, such as acute myeloid leukemia (AML) cells [17], bovine mammary epithelial (MAC-T) cells [18] and oligodendrocyte cells [19]. Sufficient studies also indicated that NF-κB signaling was activated in the process of myocardial I/R injury, and inhibition of NF-κB signal reduced myocardial apoptosis, further alleviating myocardial I/R injury [7, 20]. Numerous studies support the involvement of EDA2R in apoptosis induction via NF-κB activation in cancer cells [21–23]. Therefore, we hypothesized that EDA2R might serve a vital role in myocardial I/R injury via NF-κB signaling. However, whether NF-κB signaling mediates the function of EDA2R in myocardial I/R injury requires further confirmation.

Dexmedetomidine (DEX) is a highly selective agonist of α2-adrenergic receptors (α2-ARs) and has been applied in clinical anesthesia and intensive care units, exerting sedative, analgesic and sympatholytic effects [24]. DEX is effective in attenuating the stress response to surgical stimulation and improving the oxygen supply-demand balance in the heart [25]. In addition, various studies have indicated that DEX exerts protective effects against I/R injury via direct action on the myocardium [26–28]. Therefore, to explore the protective effects of DEX, we screened downstream factors regulated by DEX through GEO database. Based on the GSE126104 profile, DEX decreases EDA2R expression in the left ventricle of rats, suggesting that EDA2R may participate in protective effects of DEX on myocardial I/R injury.

The present study aimed to explore the role and mechanism of EDA2R during myocardial I/R injury using *in vivo* and *in vitro* experiments.

Materials and Methods

Cell culture and hypoxia/reoxygenation (H/R) model

AC16 human cardiomyocytes were purchased from iCell Bioscience Inc. (Shanghai, China). Cells were cultured in GibcoDulbecco's Modified Eagle Medium/F12 (DMEM/F12, Procell Life Science & Technology Co., Ltd., Wuhan, China) containing 10% fetal bovine serum (FBS, Tianhang Biotechnology Co., Ltd., Zhejiang, China) at 37°C in a 5% CO_2 incubator.

H/R cells were cultured under hypoxic conditions (1% O_2; 5% CO_2; 94% N_2) for 16 h and then returned to normal oxygen conditions for 2 h. Control cells were cultured under normal oxygen conditions for 18 h. At 1 h before culture under H/R conditions, 1 μM DEX (BL171A, Biosharp Biotech Co., Ltd., Hefei, China) was added to H/R+DEX cells and cells were treated for 19 h.

Transfection

The pRNAH1.1 vector was obtained from GenScript (Piscataway, NJ, USA). According to the experimental groups, AC16 cells were inoculated into 6-well plates (4×10^5 per well) and cultured at 37°C in a 5% CO_2 incubator. Transfection was carried out after cell adherence. The short hairpin RNA (shRNA-1) sequence (GGAGACAGGCTGGAGCTCAATTCAAGAGATTGAGCTCCAGCCTGTCTCTTTTT) and shRNA-2 sequence (GGCAGTTTGAGGCTGATAAATTCAAGAGATTTA TCAGCCTCAAACTGCTTTTT) targeting EDA2R or negative control (NC) sequence (GTTCTCCGAACGTGTCACGTTTCAAGAGAACGTGACACGTTCGGAGAATTTTT) were inserted into the pRNAH1.1 vector. Subsequently, the plasmids were transfected into AC16 cells using Lipofectamine 3000 (Invitrogen, Thermo Fisher Scientific Inc., Carlsbad, MA, USA). After transfection for 24 h, the cells were cultured under hypoxic conditions for 16 h and then under normal oxygen conditions for 2 h. Afterwards, cells were collected for subsequent experiments.

Establishment of a mouse myocardial I/R model and adeno-associated virus infection

All animal experiments were carried out in accordance with the National Institutes of Health Guide for the Care and Use of Laboratory Animals. The study protocol was approved by Harbin Children's Hospital Ethical Medical Committee (2023-IEC-01). Male C57BL/6 mice (8–10 weeks old, 25 g) were obtained from Liaoning Changsheng Biotechnology Co., Ltd. (Benxi, China). They were randomly divided into four groups: Sham, I/R, I/R + adeno-associated virus 9 (AAV9)-NC and I/R+AAV9-shEDA2R (n=24 per group). The shRNA sequence targeting EDA2R was CCGGGATTGTGGTTATGGAGAAGGTTCAAGAGACCTTCTCCATAACCACAATCCTTTTTT. After 1 week of adaptive feeding, the mouse myocardial I/R model was established by ligation of the left anterior descending branch (ligation for 30 min and reperfusion for 24 h) according to the previously reports [29, 30]. Briefly, after thoracotomy, the capsule was cut to expose the left atrial appendage, and the heart was gently pinched out of the pore. At the lower margin of the left atrial appendage 1–2 mm and next to the pulmonary conus 0.5 mm, a 5-0 suture needle was ligation through the anterior descending coronary artery with a needle width of about 2 mm. Sham mice received thoracotomy without ligation. I/R + AAV9-NC and I/R + AAV9-shEDA2R mice were injected with control or shEDA2R AAV9 (1×10^{11}v.g, 125 μl) via the caudal vein 10 days before I/R model establishment. After 24 h, myocardial ultrasound was performed to evaluate the left ventricular functions, including the left ventricular end systolic diameter (LVESD), left ventricular end-systolic volume (LVESV), left ventricular end diastolic dimension (LVEDD), left ventricular end-diastolic volume (LVEDV), LVEF (= LVEDV − LVESV / LVESV × 100%) and LVFS (= LVEDD − LVESD / LVESD × 100%). After ultrasound, all experimental mice were euthanized by CO_2 asphyxiation (flow rate, 60% of the chamber volume/min). The basal myocardial tissues from the free wall of the left heart in myocardial infarction areas were collected for the follow-up experiments.

Cell -Counting Kit 8 (CCK-8) assay

AC16 cells were seeded into 96-well plates at a density of 5×10^3 cells per well. CCK-8 reagent (10 μl; KeyGen Biotech Co., Ltd., Nanjing, China) was added into each well and cells were incubated for 2 h at 37°C. Optical density values at 450 nm were measured on a microplate reader (BioTek; Agilent Technologies, Inc., Winooski, VT, USA).

Flow cytometry

According to the manufacturer's instructions, cardiomyocytes were centrifuged 150 × g at room temperature for 5 min and collected. After removing the supernatant, cardiomyocytes were washed twice with PBS and suspended with 500 μl Binding Buffer. Subsequently, cells were treated with 5 μl Annexin V-FITC and 5 μl PI, and incubated at room temperature for 5–10 min in the dark. A NovoCyte flow cytometer (ACEA Bioscience Inc., San Diego, CA, USA) was used to detect apoptosis.

Transmission electron microscopy

AC16 cells fixed at 4°C were rinsed with 0.1 M phosphate buffer PB (PH7.4), and then dehydrated with 30%-50%-70%-80%-95%-100%-100% alcohol for 20 min each time, and 100% acetone twice for 15 min each time. The cells were permeated with 812 embedding agents overnight at 37°C. After polymerization for 48 h at 60°C, the cells were embedded using resin block and resin block were cut into ultrathin slices of 60–80 nm. The slices were stained with 2% uranyl acetate saturated alcohol solution for 8 min and 2.6% lead citrate solution for 8 min in the dark. The staining was observed under transmission electron microscope (Hitachi, Tokyo, Japan).

JC-1 staining

For mitochondrial membrane potential (MMP) detection, AC16 cells were incubated with JC-1 for 20 min at 37°C. After incubation, the supernatant was removed and cells were treated with JC-1 dyeing buffer (1X). Subsequently, the images for JC-1 monomers (green fluorescence) and JC-1 aggregates (red fluorescence) were captured under a fluorescence microscope (Olympus, Tokyo, Japan).

Immunofluorescence

Cell slides were fixed with 4% paraformaldehyde for 15 min at room temperature. Subsequently, slides were permeabilized using 0.1% Triton X-100 and washed in PBS. After blocking using 1% BSA (Sangon Biotech Co., Ltd., Shanghai, China), the slides were incubated with anti-NF-κB p65 (dilution, 1:100; A2547; ABclonal Biotech Co., Ltd., Wuhan, China) overnight at 4°C. Secondary antibody goat anti-rabbit IgG (dilution, 1:200; A27039; Invitrogen, Thermo Fisher Scientific Inc.) was added to the slides and slides were incubated at room temperature for 60 min. Nuclei were counterstained with DAPI (Aladdin Biochemical Technology Co., Ltd., Shanghai, China). Cells were observed under a fluorescence microscope.

Electrophoretic mobility shift assay (EMSA)

Nuclear protein was isolated using a Nuclear Protein Isolation Kit (Beyotime, Shanghai, China). The protein concentration was examined using a BCA protein concentration assay kit (Beyotime). The EMSA binding reaction was performed in line with the protocol of EMSA kit (Beyotime). Briefly, protein extracts were mixed with biotin-labeled NF-κB probe and incubated at room temperature for 10 min. After electrophoresis, samples were transferred to a membrane for 40 min and cross-linked for 10 min. ECL Plus Reagent solution was used for detection of the biotin-labeled probe (NF-κB).

H&E staining

I/R-induced myocardial histopathological changes were visualized using H&E staining. The embedded myocardial tissues were cut into 5-μm slices, and dewaxed and hydrated in xylene and ethanol. Subsequently, sections were stained with hematoxylin for 5 min and then eosin for 3 min. Images were obtained using a microscope.

Triphenyl tetrazolium chloride (TTC) staining

TTC was dissolved with 0.01 M PBS to prepare a 2% staining solution. The myocardial tissues were sliced. TTC staining solution (2 ml) was added to the slices and slices were incubated at 37°C in the dark. After 15 min, slices were turned over and stained for 15 min. Finally, images of the staining results were captured under a microscope. The infarct area and left ventricular area of each slice of myocardia were measured using Image pro-Plus 6.0 software (Media Cybernetics, Bethesda, MD, USA). Briefly, each slice of the heart was completely outlined. "Count and measure objects" were used to output the result. The percentage of the infarct area (infarct weights/whole heart weights × 100%) was also calculated.

TUNEL staining

Paraffin-embedded myocardial tissues were sliced, dewaxed and rehydrated. After penetration using 0.1% Triton X-100 (50 μl; Beyotime), the prepared TUNEL reaction solution (50 μl) was added to the sections and the sections were incubated at 37°C for 1 h. Sections were then stained with DAPI for 5 min, and images were captured under a microscope.

Detection of oxidative stress index

Cell precipitates were re-suspended with PBS, and the protein content was determined after ultrasonic lysis. Protein concentration was measured by a BCA protein assay kit (Beyotime). Malondialdehyde (MDA) content was determined using the MDA kit (Jiancheng). Briefly, after the reagents provided by MDA kit were successively added to the samples, then samples were centrifuged for 10 min. The absorbance of the supernatant was measured at 532 nm. MDA content (nmol / mgprot) = (measured OD value − control OD value) / (Standard OD value − blank OD value) × standard tube concentration (10 nmol/ml) / protein concentration to be measured (mgprot/ml). Superoxide dismutase (SOD) activity was measured using the SOD kit (Jiancheng). The absorbance of the supernatant was measured at 570 nm. SOD activity (U / mgprot) = (control OD value − measured OD value) / control OD value) / 50% × (total volume of reaction liquid (ml) / sample size (ml) / Protein concentration of sample to be measured (mgprot/ml). According to the instructions of the reactive oxygen species (ROS) kit (Jiancheng), the dichlorodihydrofluorescein diacetate (DCFH-DA) probe was used to detect ROS levels. After incubation at 37°C for 30 min, single-cell suspension was collected. Subsequently, the supernatant was discarded and re-suspended with PBS. The excitation light was 488 nm and the emission light was 525 nm. Finally, the results were expressed as relative fluorescence intensity.

Detection of Caspase-3 and Caspase-9 activity

The activity of Caspase-3 and Caspase-9 in cardiomyocytes was detected using the corresponding kits (Beyotime) in accordance with the manufacturer's instructions.

RT-qPCR

Total RNA was extracted from cardiomyocytes. Reverse transcription of RNA into cDNA was performed using reverse transcriptase (BeyoRT II M-MLV; Beyotime). qRT-PCR amplification was performed using a SYBR green kit (Solarbio Science & Technology Co., Ltd., Beijing, China) and samples were analyzed using an ExicyclerTM96 PCR reaction system (Bioneer, Daejeon, Korea). β-actin served as an internal control for mRNA normalization. The relative RNA level of a gene was determined using by the $2^{-\Delta\Delta CT}$ method [31]. The sequences of primers used were as follows:

EDA2R forward, 5′-TTCTACCGAAAGACACGC-3′;

EDA2R reverse, 5′-GCTCAACTGGAAGGCAC-3′;

β-actin forward, 5′-CACTGTGCCCATCTACGAGG-3′;

β-actin reverse, 5′-TAATGTCACGCACGATTTCC-3′.

Western blotting

Myocardial tissues or cardiomyocytes were lysed using RIPA lysis buffer containing 1 mmol/l PMSF (Beyotime). The lysates were centrifuged at 10,000 × g for

10 min at 4°C and the clarified protein concentration was measured using a BCA protein assay kit (Beyotime). Equal amounts (30 μg) of proteins were electrophoresed on 10% SDS polyacrylamide gels, and simultaneously transferred to polyvinylidene difluoride membranes. After blocking, the membranes were incubated with primary antibodies overnight at 4°C. After washing with 5% TBST, the membranes were incubated with the corresponding secondary antibodies (goat anti-rabbit IgG, 1:10,000; SA00001-2; Proteintech, Wuhan, China or goat anti-mouse IgG, 1:10,000, SA00001-1; Proteintech) at a dilution of at 37°C for 40 min. The protein bands were visualized with ECL luminous solution (7 Sea biotech, Shanghai, China) and semi-quantified using Gel-Pro-Analyzer software 4 (Media Cybernetics).

The primary antibodies used in the present study were as follows: EDA2R antibody (1:5,000; ab167224; Abcam, Shanghai, China), Cytochrome C antibody (1:1,000; AF0358; Affinity Biosciences, Changzhou, China), Bcl-2 antibody (1: 500; A0208; ABclonal Biotech Co., Ltd., Wuhan, China), Bax antibody (1:500; A19684; ABclonal Biotech Co., Ltd.), phosphorylated IκBa antibody (1:1,000; AP0707; ABclonal Biotech Co., Ltd.), IκBa antibody (1:1,000; A1187; ABclonal Biotech Co., Ltd.), phosphorylated p65 antibody (1:1,000; AP0475; ABclonal Biotech Co., Ltd.) and p65 antibody (1:500; A2547; ABclonal Biotech Co., Ltd.).

Statistical analysis

All data were analyzed using Prism 8.0 software (GraphPad, San Diego, CA, USA) and are presented as the mean ± SD. Data between two groups were analyzed with the unpaired *t*-test. Comparisons between groups were performed using one-way or two-way analysis of variance (ANOVA), and multiple comparisons were performed with the Tukey test. $P<0.05$ was considered to indicate a statistically significant difference.

Results

DEX has a protective effect on H/R induced cardiomyocyte injury

To verify the cardioprotective effects of DEX against I/R injury, an H/R cell model was established. Firstly, cell viability was examined using a CCK-8 assay, and the data indicated that H/R significantly decreased the viability of cardiomyocytes compared with the control group, while DEX restored the cell viability inhibited by H/R (Fig. 1A). Furthermore, to elucidate the effect of DEX on apoptosis in AC16 cells exposed to H/R, flow cytometry was performed. H/R increased the number of apoptotic cardiomyocytes cells, triggering cell apoptosis. However, DEX decreased the apoptotic rate of cardiomyocytes, reversing the effects of H/R on apoptosis (Figs. 1B and C). Results of GSE126104 chip showed that DEX decreased EDA2R expression in the left ventricle of rats (Fig. 1D). In addition, RT-qPCR and western blotting analysis were used to assess the mRNA and protein levels of EDA2R in cardiomyocytes treated with DEX. Notably, as shown in Fig. 1E, DEX markedly decreased EDA2R expression in a H/R cell model. Taken together, the aforementioned findings suggested that DEX attenuated H/R-induced cardiomyocyte injury, and EDA2R might be involved in the protective effects of DEX during the I/R process.

EDA2R knockdown suppresses H/R-induced cardiomyocyte apoptosis

Firstly, shEDA2R-1 and shEDA2R-2 were transfected into AC16 cells to analyze the effect of EDA2R knockdown on cardiomyocyte apoptosis. The results of RT-qPCR and western blotting demonstrated that EDA2R expression was significantly downregulated in H/R+shEDA2R cells compared with the H/R+shNC cells, indicating successful transfection (Fig. 2A). To determine the effects of EDA2R silencing on cell viability, a CCK-8 assay was performed. The results demonstrated that H/R decreased cell viability, and knockdown of EDA2R reversed this phenotype, while shNC transfection did not (Fig. 2B). With respect to cardiomyocyte apoptosis, the results of flow cytometry shown in Figs. 2C and D suggested that H/R triggered an increase in the number of apoptotic cardiomyocytes, while EDA2R knockdown deceased the apoptosis rate, abolishing the promoting effects of H/R on apoptosis. Collectively, these data indicated that knockdown of EDA2R suppressed H/R-induced cardiomyocyte apoptosis.

EDA2R knockdown represses mitochondria-mediated apoptosis

To further verify the effect of EDA2R knockdown in mitochondria-mediated apoptosis, the mitochondrial morphology of cardiomyocytes was first observed by transmission electron microscopy. As shown in Fig. 3A, mitochondria in the control group exhibited standard reniform structure with complete morphology and clear cristae. Mitochondria in the H/R cells were shriveled and vacuolated, and the cristae were fuzzy. In addition, mitochondrial morphology in the EDA2R knockdown group was restored, which suggested that EDA2R knockdown repaired the mitochondrial morphology destroyed by H/R. Furthermore, to identify the molecular basis of apoptosis suppression by shEDA2R, the changes in MMP were determined using JC-1 staining. As shown

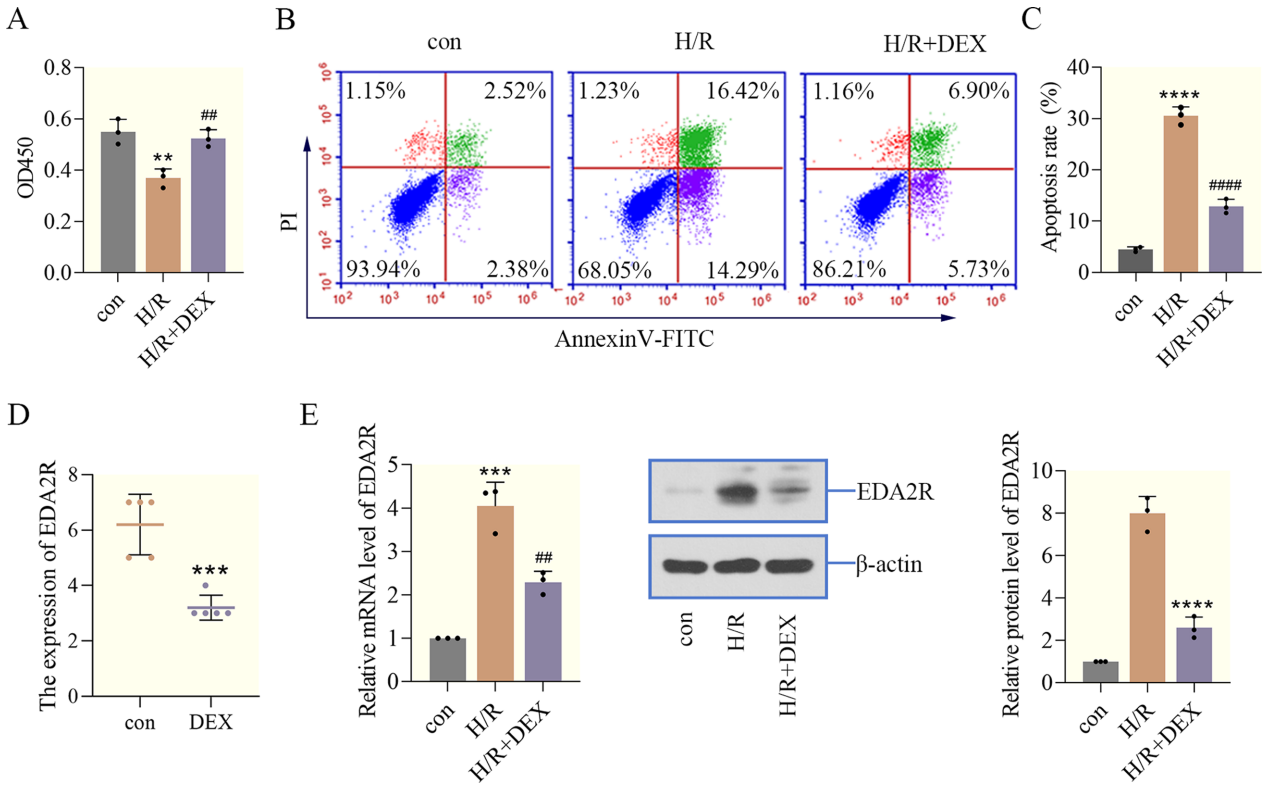

Fig. 1. Dexmedetomidine (DEX) has a protective effect on hypoxia/reoxygenation (H/R)-induced cardiomyocyte injury. (A) Cell -Counting Kit 8 (CCK-8) was used to measure cell viability. (B, C) Apoptosis and apoptotic rate were determined using flow cytometry. (D) GSE126104 showed that DEX decreased ectodysplasin-A2 receptor (EDA2R) expression in the left ventricle of rats. ***, P<0.001 vs. con. (E) The expression of EDA2R in cardiomyocytes was detected by RT-qPCR and western blotting. **P<0.01; ***P<0.001; ****P<0.0001 vs. con. $^{\#\#}P$<0.01; $^{\#\#\#\#}P$<0.0001 vs. H/R. n=3.

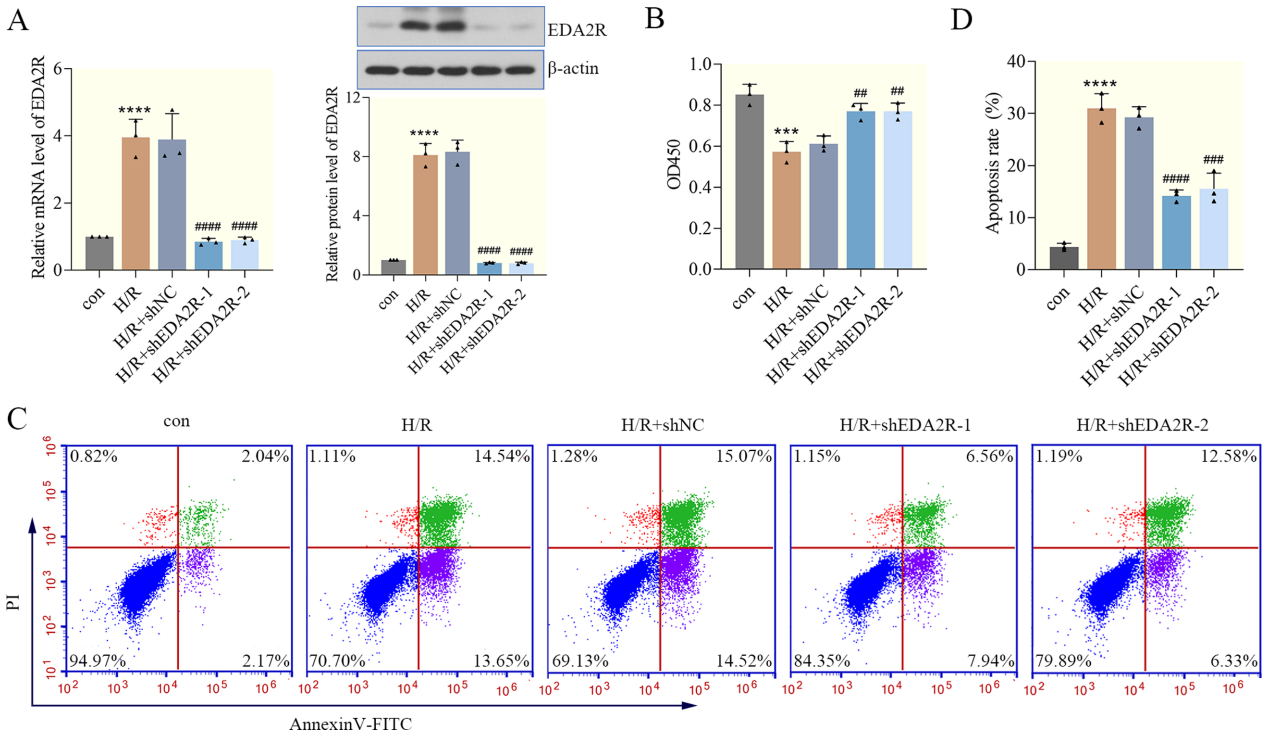

Fig. 2. Ectodysplasin-A2 receptor (EDA2R) knockdown suppresses hypoxia/reoxygenation (H/R)-induced cardiomyocyte apoptosis. (A) The knockdown efficiency of EDA2R in cardiomyocytes was detected by RT-qPCR and western blotting. (B) Cell -Counting Kit 8 (CCK-8) was applied to detect cell viability. (C, D) Apoptosis was determined using flow cytometry, and apoptotic rate was calculated. ***P<0.001; ****P<0.0001 vs. con. $^{\#\#}P$<0.01; $^{\#\#\#}P$<0.001; $^{\#\#\#\#}P$<0.0001 vs. H/R+shNC. n=3.

in Fig. 3B, the MMP in H/R-treated cardiomyocytes was decreased, while that in EDA2R knockdown-treated cardiomyocytes was significantly increased. In addition, the present study examined the release of Cytochrome C (a component of the electron transport chain in mitochondria). H/R increased cytoplasmic Cytochrome C levels and decreased mitochondrial Cytochrome C levels, indicating that the integrity of the mitochondria was impaired, while EDA2R knockdown reversed these alterations caused by H/R (Figs. 3C and D).

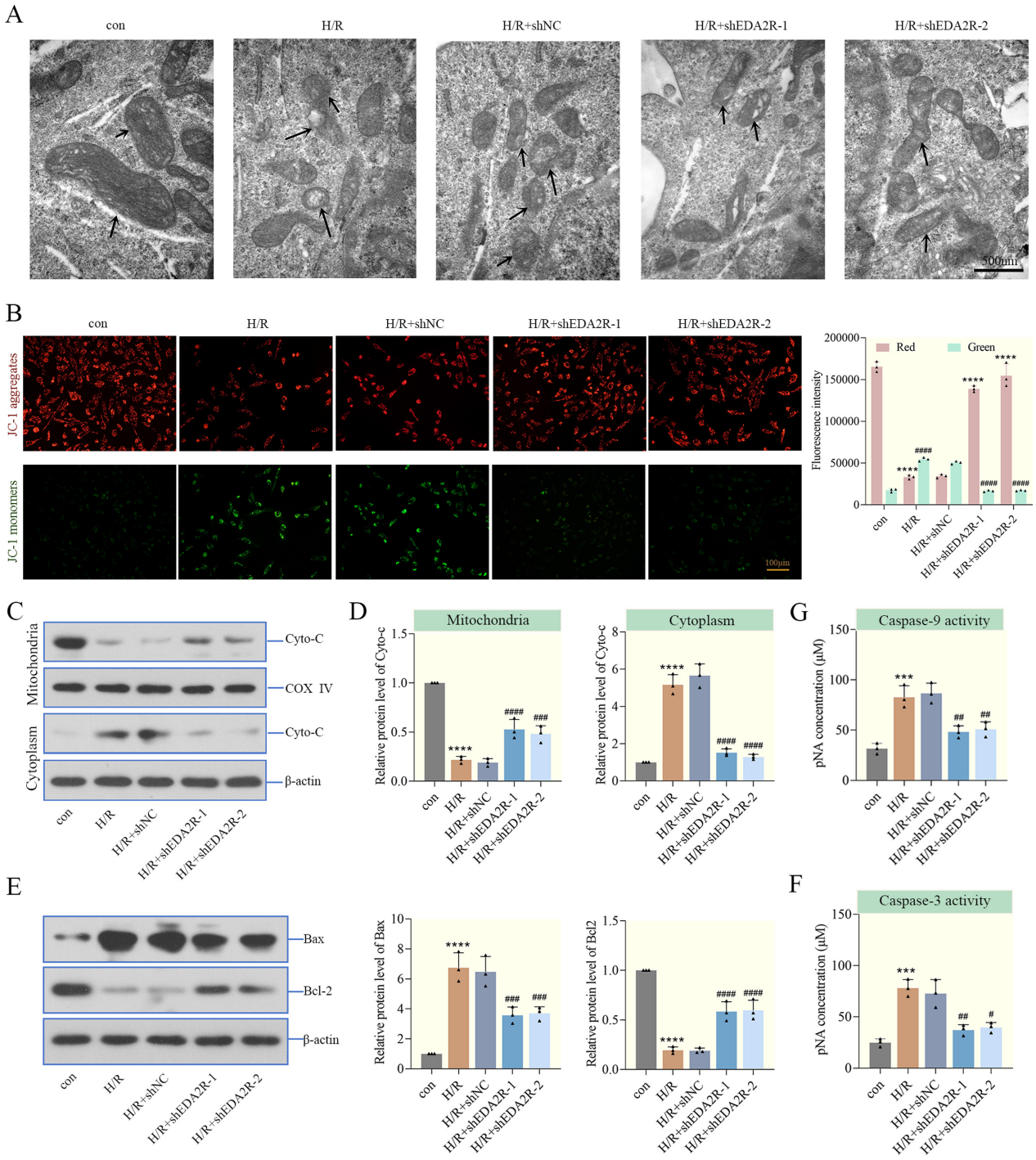

Fig. 3. Ectodysplasin-A2 receptor (EDA2R) knockdown represses mitochondria-mediated apoptosis. (A) Mitochondrial morphology of cardiomyocytes was observed by transmission electron microscopy (the arrows represented mitochondrial morphology, scale bar=500 nm). (B) Mitochondrial membrane potential (MMP) was detected by JC-1 (Scale bar=100 μm, Red: ****P<0.0001 vs. con. or hypoxia/reoxygenation (H/R)+shNC; Green: $^{\#\#\#\#}P$<0.0001 vs. con. H/R+shNC). (C, D) The levels of cytochrome C in mitochondria and cytoplasm of cardiomyocytes were determined by western blotting. (E) The expressions of Bax and Bcl-2 were determined in cardiomyocytes by western blotting. (F, G) Caspase-3 and Caspase-9 activity in cardiomyocytes was detected. ***P<0.001; ****P<0.0001 vs. con. $^{\#}P$<0.05; $^{\#\#}P$<0.01; $^{\#\#\#}P$<0.001; $^{\#\#\#\#}P$<0.0001vs. H/R+shNC. n=3.

To investigate the possible role of EDA2R knockdown in apoptosis, the levels of apoptosis-related factors were detected in cardiomyocytes. The levels of apoptosis-associated proteins were markedly altered after H/R administration. As shown in Figs. 3E–G, H/R markedly increased Bax levels, Caspase-3 and Caspase-9 activity, and decreased Bcl-2 levels. EDA2R knockdown showed opposite function. These findings demonstrated that knockdown of EDA2R repressed mitochondria-mediated apoptosis in cardiomyocytes.

EDA2R knockdown relieves H/R-induced oxidative stress

To determine the effect of EDA2R knockdown on oxidative stress, the index related to oxidative stress was measured. As suggested in Figs. 4A and B, H/R increased the MDA content and decreased SOD activity in cardiomyocytes, indicating that oxidative stress occurred following H/R injury. Of note, the aforementioned effects were markedly abolished by EDA2R knockdown. Additionally, to investigate whether EDA2R knockdown affects ROS, cardiomyocytes were stained with DCFH-DA and ROS production was detected. As expected, the results of flow cytometry confirmed that, in contrast to H/R, EDA2R knockdown caused a significant decrease in ROS production (Fig. 4C). Based on these observations, knockdown of EDA2R relieved H/R-induced oxidative stress in cardiomyocytes.

EDA2R knockdown inhibits the activation of the NF-κB signaling pathway

We hypothesized that EDA2R served a key role in the process of cardiac I/R injury by regulating NF-κB signaling. Therefore, western blotting analysis was carried out to determine the levels of IκBα, p-IκBα, NF-κB p65 and p-NF-κB p65 in cardiomyocytes. The results in Fig. 5A demonstrated that the levels of these proteins were markedly changed after H/R. H/R decreased IκBα levels, and enhanced the phosphorylation of IκBα and NF-κB p65. However, EDA2R knockdown decreased the phosphorylation of IκBα and NF-κB p65, reversing the effects of H/R on NF-κB signaling. Moreover, analysis of immunofluorescence staining and the EMSA indicated that H/R increased the nuclear translocation of NF-κB p65 and the specificity binding of NF-κB, which was markedly abolished by EDA2R knockdown (Figs. 5B and C). These results provided evidence that EDA2R knockdown inhibited the activation of the NF-κB signaling pathway in cardiomyocytes, thus alleviating H/R-induced I/R injury.

EDA2R knockdown weakens myocardial I/R injury in mice

To examine the effect of EDA2R on I/R-treated hearts, a mouse myocardial I/R model was established and EDA2R expression was decreased using an adeno-associated virus system (Fig. 6A). Firstly, the left ventricular function was measured in mice after I/R injury. Our data showed that the LVESD, LVESV, LVEDV and LVEDD were significantly increased and the LVEF and LVFS was decreased after I/R. Mice with EDA2R knockdown exhibited significantly improved cardiac function during reperfusion (Fig. 6B), supporting a protective role of EDA2R knockdown in mice suffering from I/R injury. Ultrasonic cardiogram of each group was shown in Fig. 6C. The heart rate slowed down in the I/R group, while it recovered in the EDA2R knockdown group (Fig. 6D). Additionally, H&E staining was used to detect histopathological changes of myocardial tissues, and the results verified that increased infarct size and histological

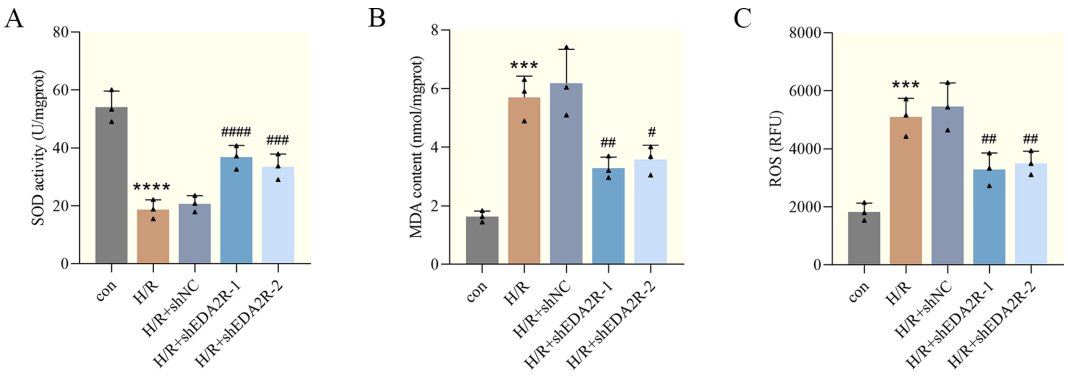

Fig. 4. Ectodysplasin-A2 receptor (EDA2R) knockdown relieves hypoxia/reoxygenation (H/R)-induced oxidative stress. (A, B) Superoxide dismutase (SOD) activity and malondialdehyde (MDA) levels in cardiomyocytes. (C) Dichlorodihydrofluorescein diacetate (DCFH-DA) probe was used to examine reactive oxygen species (ROS) levels in cardiomyocytes. ***P<0.001; ****P<0.0001 vs. con. $^{\#}P$<0.05; $^{\#\#}P$<0.01; $^{\#\#\#}P$<0.001; $^{\#\#\#\#}$, P<0.0001 vs. H/R+shNC. n=3.

damage were observed after I/R, while EDA2R knockdown alleviated it, exhibiting cardioprotective effects (Fig. 6E). I/R also increased heart weight, whereas EDA2R knockdown decreases it (Fig. 6E). TTC staining confirmed that I/R led to myocardial infarction, while EDA2R knockdown reduced the infarct size and percentage of infarct size, thus weakening I/R injury (Fig. 6F). Furthermore, apoptosis was detected by TUNEL and JC-1 staining. The results in Figs. 6G and H showed that TUNEL-positive cells were increased and the MMP was decreased in I/R mice, while EDA2R-knockdown mice exhibited the opposite phenotype, implying that EDA2R knockdown largely decreased I/R-induced apoptosis. Similarly, I/R mice exhibited a notable increase in MDA content and ROS levels, as well as a decrease in SOD activity (Fig. 6I). The opposite results were obtained in the EDA2R knockdown group (Fig. 6I). Additionally, EDA2R knockdown reversed the increase in nuclear NF-κB p65 levels following I/R, thus inhibiting the activation of the NF-κB signaling pathway (Fig. 6J). In

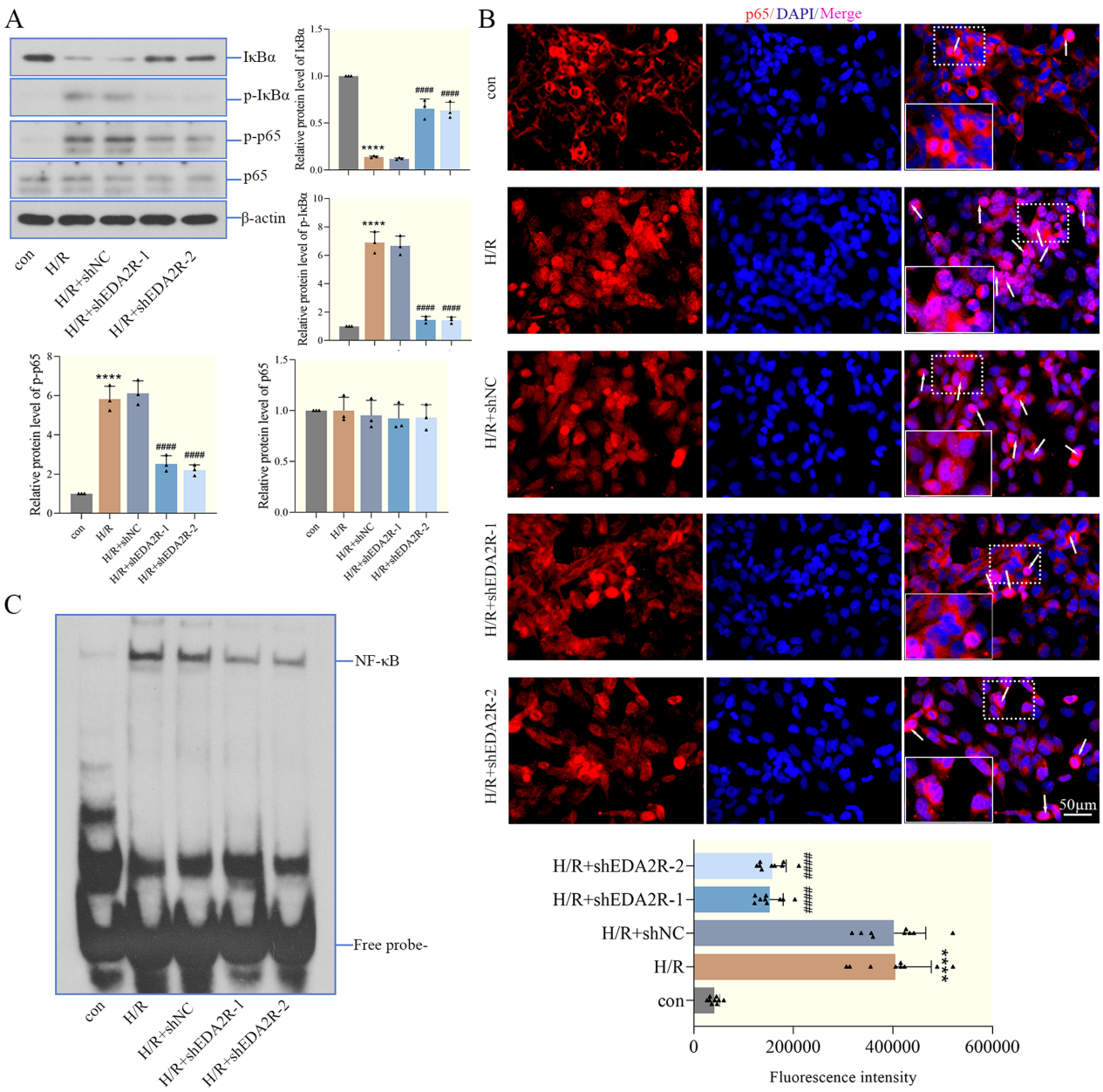

Fig. 5. Ectodysplasin-A2 receptor (EDA2R) knockdown inhibits the activation of the NF-κB signaling pathway. (A) The levels of IκBα, p-IκBα (Ser32), NF-κB p65 and p-NF-κB p65 (Ser536) were detected in cardiomyocytes by western blotting. (B) The expression distribution of NF-κB p65 in cardiomyocytes was determined by immunofluorescence, the fluorescence intensity of p65 in the nucleus was quantified in three fields of three sections (the arrows represented the distribution of p65 in the nucleus, scale bar=50 μm). (C) The transcriptional activity of NF-κB in cardiomyocytes was measured by the electrophoretic mobility shift assay (EMSA). ****P<0.0001 vs. con. $^{\#\#\#\#}P$<0.0001. n=3.

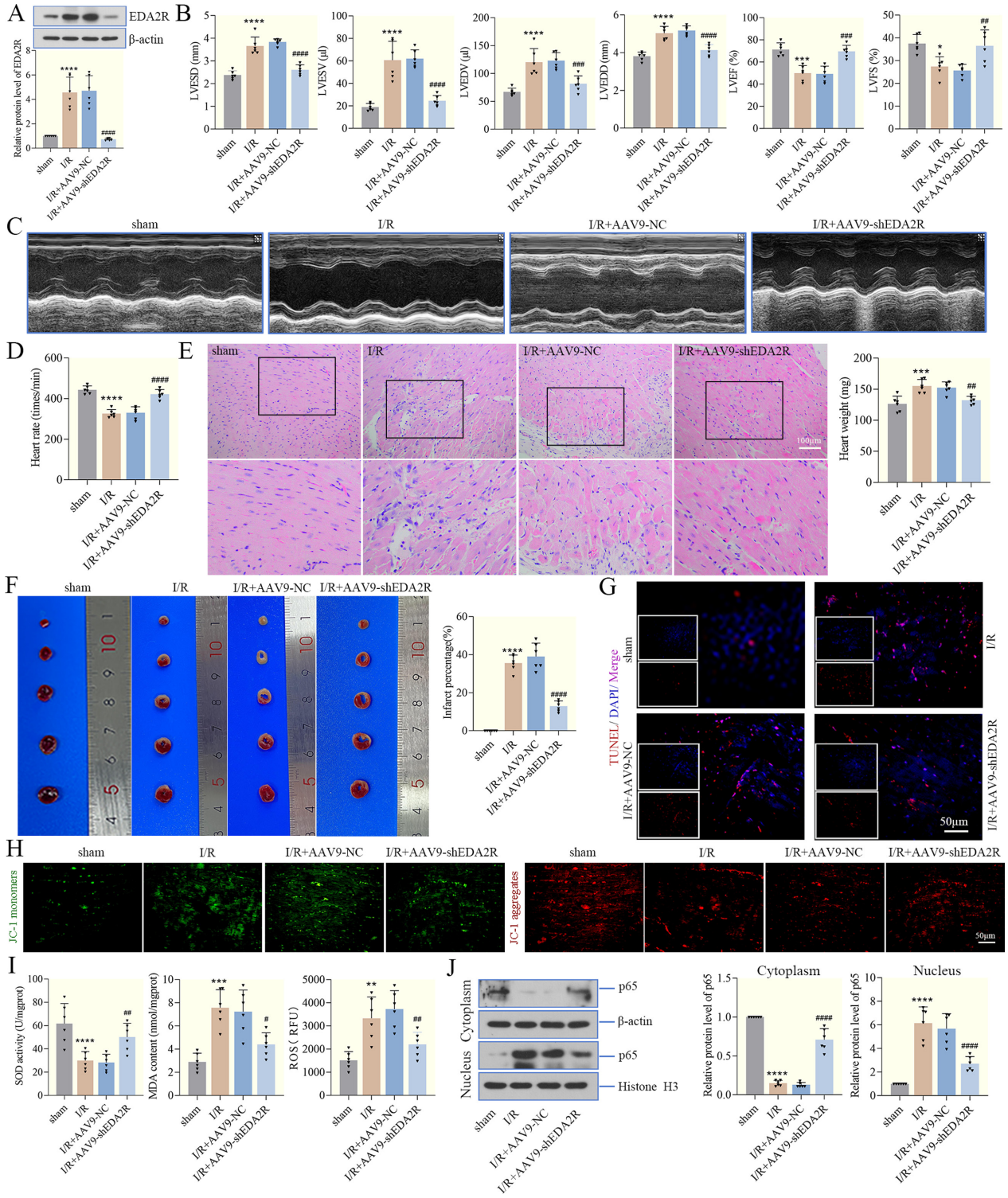

Fig. 6. Ectodysplasin-A2 receptor (EDA2R) knockdown weakens myocardial ischemia/reperfusion (I/R) injury in mice. (A) The knockdown efficiency of EDA2R was determined by western blotting. (B, C) The left ventricular end systolic diameter (LVESD), left ventricular end-systolic volume (LVESV), left ventricular end-diastolic volume (LVEDV), left ventricular end diastolic dimension (LVEDD), LVEF and LVFS were evaluated, and representative echocardiograms were presented. (D) Heart rate in each group. (E) H&E staining was used to detect histopathological changes of myocardial tissues (Scale bar=100 μm). Heart weight was also measured. (F) The infarct size was determined by triphenyl tetrazolium chloride (TTC) staining, and infarct percentage was measured. (G) Myocardial tissue apoptosis was detected by TUNEL staining (Scale bar=50 μm). (H) mitochondrial membrane potential (MMP) was determined by JC-1 in myocardial tissues (Scale bar=50 μm). JC-1 monomer and dimer were the same cell samples and field of view for each experimental condition. (I) Superoxide dismutase (SOD) activity and malondialdehyde (MDA) levels in myocardial tissues. Dichlorodihydrofluorescein diacetate (DCFH-DA) probe was used to examine reactive oxygen species (ROS) levels in myocardial tissues. (J) The levels of cytoplasmic NF-κB p65 and nuclear NF-κB p65 in myocardial tissues were detected by western blotting. *P<0.05; **P<0.01; ***P<0.001; ****P<0.0001 vs. sham. $^{\#}P$<0.05; $^{\#\#}P$<0.01; $^{\#\#\#}P$<0.001; $^{\#\#\#\#}P$<0.0001 vs. I/R + adeno-associated virus 9 (AAV9) − NC. n=6.

summary, these data confirmed that knockdown of EDA2R weakened myocardial I/R in mice, consistent with the *in vitro* results.

Discussions

I/R injury is the leading cause of death and morbidity in patients with ischemic heart disease, and effective clinical therapies for the prevention or treatment of myocardial I/R injury are still lacking [32, 33]. Multiple mechanisms are involved in myocardial I/R injury, such as inflammation, apoptosis and ROS [34]. Notably, GEO database results indicated that EDA2R expression was elevated in the myocardial tissues of a mouse myocardial I/R model. Furthermore, the cardioprotective properties of DEX have been confirmed in several studies [35–37]. For example, Yang *et al.* suggested that DEX pretreatment protected the hearts against I/R injury by inhibiting inflammation and apoptosis [38]. Based on analysis of the GEO database and the present study, DEX downregulated EDA2R expression in the left ventricle of rats and cardiomyocytes, suggesting that EDA2R might be involved in the protective effects of DEX on myocardial I/R injury. Thus, an H/R cell model was established and EDA2R expression was knocked down to identify the effect of EDA2R knockdown on myocardial I/R injury.

Apoptosis has been demonstrated to exert an important role in I/R-induced tissue damage [39]. A study suggests that I/R-induced apoptosis increases cardiomyocyte injury severity, which is associated with cardiomyocyte death [40]. EDA2R has been shown to be associated with tumor progression and metabolic diseases [41]. Sufficient studies have indicated that EDA2R mediates apoptosis in numerous cell types [6, 23, 42]. For instance, EDA2R has been implicated in isoform EDA-A2-induced apoptosis of hair follicle cells [6] and osteosarcoma cells [43]. Furthermore, silencing of EDA2R enhanced the viability and reduced the apoptosis of hyperoxia-induced murine lung epithelial cells [12]. The present findings suggested that EDA2R knockdown increased cell viability and suppressed H/R-induced cardiomyocyte apoptosis. Additionally, H/R-induced mitochondrial dysfunction and apoptosis are responsible for the exacerbation of myocardial I/R injury [44]. We also demonstrated that EDA2R knockdown repaired H/R-destroyed mitochondrial morphology and further increased the MMP. It is also well known that cytochrome C is essential for apoptosis and released from the mitochondria to the cytosol [45]. It can cleave and activate the key executioner Caspase-3 or Caspase-9, resulting in apoptosis [46]. Our results demonstrated that EDA2R knockdown markedly decreased cytoplasmic Cytochrome C levels and increased mitochondrial Cytochrome C levels. Additionally, EDA2R knockdown decreased Bax levels, Caspase-3 and Caspase-9 activity, and increased Bcl-2 levels, further suppressing mitochondria-mediated apoptosis and restoring mitochondrial integrity. Following on from these findings, the present study demonstrated that inhibition of EDA2R relieved myocardial I/R injury, in accordance with the aforementioned studies.

Oxidative stress caused by massive ROS production induced by I/R is an important pathogenesis of I/R [47]. Therefore, inhibition of oxidative stress may effectively alleviate I/R injury and cell death. MDA is an end-product of lipid peroxidation, while SOD is an enzyme for scavenging ROS, and they both reflect the lipid peroxidation degree [48]. Of note, in this work, EDA2R knockdown group also exerted anti-oxidative effects during I/R injury, which was manifested by increased MDA content and decreased SOD activity. Furthermore, the concomitant excessive ROS production that occurs during reperfusion causes additional damage to the heart, contributing to the expansion of the infarct size and the deterioration of myocardial function [49]. Lan *et al.* indicated that silencing of EDA2R inhibited high glucose-induced accumulation of ROS and apoptosis of podocytes [11]. We also confirmed that knockdown of EDA2R caused a marked decrease in ROS production. Based on these observations, knockdown of EDA2R relieved H/R-induced oxidative stress.

Activation of NF-κB is the main factor that determines the degree of cardiac injury [7, 50]. Additionally, NF-κB also influences cell survival and induces either pro-apoptotic or anti-apoptotic genes [51]. Accumulating evidence has indicated that EDA2R is involved in activation of the NF-κB signaling pathway [21–23, 52]. For example, Jia *et al*. indicated that knockdown of EDA2R alleviated hyperoxia-induced lung epithelial cell injury by inhibiting NF-κB pathway [12]. In addition, Verhelst *et al*. suggested that EDA2R activated the non-canonical NF-κB pathway [53]. These reports were similar to our results. Likewise, in this work, we explored the molecular mechanism of EDA2R during the process of myocardial I/R injury. Our findings revealed that knockdown of EDA2R decreased the phosphorylation of IκBα and p65 in cardiomyocytes, suggesting that loss of EDA2R might suppressed the activation of the NF-κB signaling pathway, thereby attenuating myocardial I/R injury. Notably, Sinha *et al*. verified that EDA2R was involved in binding to TRAF3 and −6 and served a major role in the activation of the NF-κB pathway [23]. We hypothesized that EDA2R activates NF-κB signaling pathway by binding to TRAF3 and −6 during myocardial I/R injury. How-

ever, this hypothesis needs further verification in the future.

Notably, a limitation of this study is that *in vivo* results are preliminary data. Our *in vivo* experiment resluts revealed that EDA2R knockdown relieved the left ventricular function, with downregulated LVESD, LVESV, LVEDV and LVEDD and upregulated LVEF and LVFS. In addition, after I/R, increased myocardial infarct sizes and histological damage were observed in I/R mice, and these effects were effectively alleviated by EDA2R knockdown. Furthermore, basal myocardial tissues from the free wall of the left heart in myocardial infarction areas were used to evaluate apoptosis, oxidative stress and so on. Our findings indicated that knockdown of EDA2R largely repressed myocardial apoptosis, oxidative stress and activation of NF-κB signaling, further potentiating its cardioprotective effects. In summary, these findings demonstrated that knockdown of EDA2R protected mice hearts from I/R damage, in line with the *in vitro* results. Therefore, future clinical studies are needed to verify the cardioprotective effects of inhibition of EDA2R in patients at risk of myocardial I/R injury.

Conclusions

The current study indicated that downregulation of EDA2R participated in the protective effects of DEX, alleviating myocardial I/R injury, which was reflected by inhibition of mitochondria-mediated cardiomyocyte apoptosis and oxidative stress via the NF-κB signaling pathway (Fig. 7). However, whether EDA2R mediates the role of DEX needs to be further verified. These findings demonstrated that EDA2R may be an important target for the treatment of myocardial I/R injury.

Funding

Not applicable.

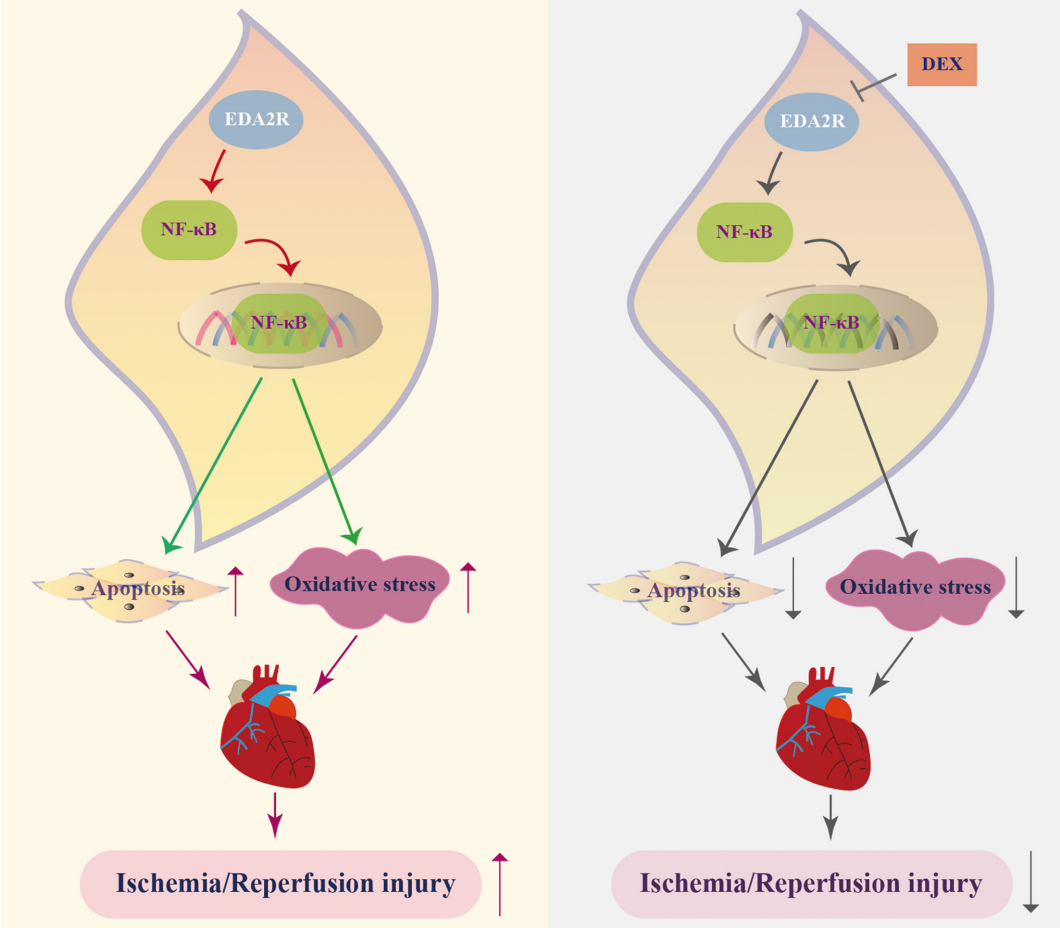

Fig. 7. A scheme of ectodysplasin-A2 receptor (EDA2R) role in myocardial ischemia/reperfusion (I/R) injury. Dexmedetomidine (DEX) downregulates the expression of EDA2R, and decreasing EDA2R inhibits the activation of the NF-κB signaling pathway, thus suppressing cell apoptosis and oxidative stress, further alleviating myocardial I/R injury.

Availability of Data and Materials

Data are available upon reasonable request.

Authors' Contributions

Guo-Nian Wang: Conceptualization and Writing − review & editing; Zhi-Hui Guan and Yi Wang: Software and Methodology; Di Yang and Jia-Bin Ma: Formal analysis; Zhi-Hui Guan: Writing − original draft. All authors read and approved the final manuscript.

Conflicts of Interest

The authors declare no potential conflicts of interest.

Acknowledgments

Not applicable.

References

1. Schwartz Longacre L, Kloner RA, Arai AE, Baines CP, Bolli R, Braunwald E, et al. National Heart, Lung, and Blood Institute, National Institutes of Health. New horizons in cardioprotection: recommendations from the 2010 National Heart, Lung, and Blood Institute Workshop. Circulation. 2011; 124: 1172–1179. [Medline] [CrossRef]
2. Yellon DM, Hausenloy DJ. Myocardial reperfusion injury. N Engl J Med. 2007; 357: 1121–1135. [Medline] [CrossRef]
3. Heusch G, Musiolik J, Gedik N, Skyschally A. Mitochondrial STAT3 activation and cardioprotection by ischemic postconditioning in pigs with regional myocardial ischemia/reperfusion. Circ Res. 2011; 109: 1302–1308. [Medline] [CrossRef]
4. Zhai M, Li B, Duan W, Jing L, Zhang B, Zhang M, et al. Melatonin ameliorates myocardial ischemia reperfusion injury through SIRT3-dependent regulation of oxidative stress and apoptosis. J Pineal Res. 2017; 63: e12419. [Medline] [CrossRef]
5. Pei H, Yu Q, Xue Q, Guo Y, Sun L, Hong Z, et al. Notch1 cardioprotection in myocardial ischemia/reperfusion involves reduction of oxidative/nitrative stress. Basic Res Cardiol. 2013; 108: 373. [Medline] [CrossRef]
6. Kwack MH, Kim JC, Kim MK. Ectodysplasin-A2 induces apoptosis in cultured human hair follicle cells and promotes regression of hair follicles in mice. Biochem Biophys Res Commun. 2019; 520: 428–433. [Medline] [CrossRef]
7. Li D, Wang X, Huang Q, Li S, Zhou Y, Li Z. Cardioprotection of CAPE-oNO$_2$ against myocardial ischemia/reperfusion induced ROS generation via regulating the SIRT1/eNOS/NF-κB pathway in vivo and in vitro. Redox Biol. 2018; 15: 62–73. [Medline] [CrossRef]
8. Yang L, Huang X, Wang W, Jiang T, Ding F. XEDAR inhibits the proliferation and induces apoptosis of gastric cancer cells by regulating JNK signaling pathway. Biosci Rep. 2019; 39: BSR20192726. [Medline] [CrossRef]
9. Sinha SK, Chaudhary PM. Induction of apoptosis by X-linked ectodermal dysplasia receptor via a caspase 8-dependent mechanism. J Biol Chem. 2004; 279: 41873–41881. [Medline] [CrossRef]
10. Kwack MH, Jun MS, Sung YK, Kim JC, Kim MK. Ectodysplasin-A2 induces dickkopf 1 expression in human balding dermal papilla cells overexpressing the ectodysplasin A2 receptor. Biochem Biophys Res Commun. 2020; 529: 766–772. [Medline] [CrossRef]
11. Lan X, Kumar V, Jha A, Aslam R, Wang H, Chen K, et al. EDA2R mediates podocyte injury in high glucose milieu. Biochimie. 2020; 174: 74–83. [Medline] [CrossRef]
12. Jia N, Jia Y, Yang F, Du W. Knockdown of EDA2R alleviates hyperoxia-induced lung epithelial cell injury by inhibiting NF-κB pathway. Allergol Immunopathol (Madr). 2022; 50: 84–90. [Medline] [CrossRef]
13. Kumar A, Takada Y, Boriek AM, Aggarwal BB. Nuclear factor-kappaB: its role in health and disease. J Mol Med (Berl). 2004; 82: 434–448. [Medline] [CrossRef]
14. Mitchell S, Vargas J, Hoffmann A. Signaling via the NFκB system. Wiley Interdiscip Rev Syst Biol Med. 2016; 8: 227–241. [Medline] [CrossRef]
15. Chen LF, Greene WC. Shaping the nuclear action of NF-kappaB. Nat Rev Mol Cell Biol. 2004; 5: 392–401. [Medline] [CrossRef]
16. van den Berg R, Haenen GR, van den Berg H, Bast A. Transcription factor NF-kappaB as a potential biomarker for oxidative stress. Br J Nutr. 2001; 86:(Suppl 1): S121–S127. [Medline] [CrossRef]
17. Bosman MC, Schuringa JJ, Vellenga E. Constitutive NF-κB activation in AML: Causes and treatment strategies. Crit Rev Oncol Hematol. 2016; 98: 35–44. [Medline] [CrossRef]
18. Fan WJ, Li HP, Zhu HS, Sui SP, Chen PG, Deng Y, et al. NF-κB is involved in the LPS-mediated proliferation and apoptosis of MAC-T epithelial cells as part of the subacute ruminal acidosis response in cows. Biotechnol Lett. 2016; 38: 1839–1849. [Medline] [CrossRef]
19. Hamanoue M, Yoshioka A, Ohashi T, Eto Y, Takamatsu K. NF-kappaB prevents TNF-alpha-induced apoptosis in an oligodendrocyte cell line. Neurochem Res. 2004; 29: 1571–1576. [Medline] [CrossRef]
20. Hamid T, Guo SZ, Kingery JR, Xiang X, Dawn B, Prabhu SD. Cardiomyocyte NF-κB p65 promotes adverse remodelling, apoptosis, and endoplasmic reticulum stress in heart failure. Cardiovasc Res. 2011; 89: 129–138. [Medline] [CrossRef]
21. Mikkola ML, Pispa J, Pekkanen M, Paulin L, Nieminen P, Kere J, et al. Ectodysplasin, a protein required for epithelial morphogenesis, is a novel TNF homologue and promotes cell-matrix adhesion. Mech Dev. 1999; 88: 133–146. [Medline] [CrossRef]
22. Bayés M, Hartung AJ, Ezer S, Pispa J, Thesleff I, Srivastava AK, et al. The anhidrotic ectodermal dysplasia gene (EDA) undergoes alternative splicing and encodes ectodysplasin-A with deletion mutations in collagenous repeats. Hum Mol Genet. 1998; 7: 1661–1669. [Medline] [CrossRef]
23. Sinha SK, Zachariah S, Quiñones HI, Shindo M, Chaudhary PM. Role of TRAF3 and -6 in the activation of the NF-kappa B and JNK pathways by X-linked ectodermal dysplasia receptor. J Biol Chem. 2002; 277: 44953–44961. [Medline] [CrossRef]
24. Gerlach AT, Murphy CV, Dasta JF. An updated focused review of dexmedetomidine in adults. Ann Pharmacother. 2009; 43: 2064–2074. [Medline] [CrossRef]
25. Yu M, Han C, Jiang X, Wu X, Yu L, Ding Z. Effect and placental transfer of dexmedetomidine during caesarean section under general anaesthesia. Basic Clin Pharmacol Toxicol. 2015; 117: 204–208. [Medline] [CrossRef]
26. Yoshitomi O, Cho S, Hara T, Shibata I, Maekawa T, Ureshino H, et al. Direct protective effects of dexmedetomidine against myocardial ischemia-reperfusion injury in anesthetized pigs. Shock. 2012; 38: 92–97. [Medline] [CrossRef]
27. Raupach A, Karakurt E, Torregroza C, Bunte S, Feige K, Stroethoff M, et al. Dexmedetomidine provides cardioprotection during early or late reperfusion mediated by different mitochondrial k+-channels. Anesth Analg. 2021; 132: 253–260. [Medline] [CrossRef]

28. Yu P, Zhang J, Ding Y, Chen D, Sun H, Yuan F, et al. Dexmedetomidine post-conditioning alleviates myocardial ischemia-reperfusion injury in rats by ferroptosis inhibition via SLC7A11/GPX4 axis activation. Hum Cell. 2022; 35: 836–848. [Medline] [CrossRef]
29. Huang C, Sharma A, Thakur R, Rai D, Katiki M, Germano JF, et al. Asporin, an extracellular matrix protein, is a beneficial regulator of cardiac remodeling. Matrix Biol. 2022; 110: 40–59. [Medline] [CrossRef]
30. Ye J, Lu S, Wang M, Ge W, Liu H, Qi Y, et al. Hydroxysafflor yellow A protects against myocardial ischemia/reperfusion injury via suppressing NLRP3 inflammasome and activating autophagy. Front Pharmacol. 2020; 11: 1170. [Medline] [CrossRef]
31. Livak KJ, Schmittgen TD. Analysis of relative gene expression data using real-time quantitative PCR and the 2(-Delta Delta C(T)) Method. Methods. 2001; 25: 402–408. [Medline] [CrossRef]
32. Hausenloy DJ, Yellon DM. Myocardial ischemia-reperfusion injury: a neglected therapeutic target. J Clin Invest. 2013; 123: 92–100. [Medline] [CrossRef]
33. Turer AT, Hill JA. Pathogenesis of myocardial ischemia-reperfusion injury and rationale for therapy. Am J Cardiol. 2010; 106: 360–368. [Medline] [CrossRef]
34. Zeng J, Jin Q, Ruan Y, Sun C, Xu G, Chu M, et al. Inhibition of TGFβ-activated protein kinase 1 ameliorates myocardial ischaemia/reperfusion injury via endoplasmic reticulum stress suppression. J Cell Mol Med. 2020; 24: 6846–6859. [Medline] [CrossRef]
35. Yoshikawa Y, Hirata N, Kawaguchi R, Tokinaga Y, Yamakage M. Dexmedetomidine maintains its direct cardioprotective effect against ischemia/reperfusion injury in hypertensive hypertrophied myocardium. Anesth Analg. 2018; 126: 443–452. [Medline] [CrossRef]
36. Bunte S, Behmenburg F, Majewski N, Stroethoff M, Raupach A, Mathes A, et al. Characteristics of dexmedetomidine post-conditioning in the field of myocardial ischemia-reperfusion injury. Anesth Analg. 2020; 130: 90–98. [Medline] [CrossRef]
37. Keating GM. Dexmedetomidine: a review of its use for sedation in the intensive care setting. Drugs. 2015; 75: 1119–1130. [Medline] [CrossRef]
38. Yang YF, Wang H, Song N, Jiang YH, Zhang J, Meng XW, et al. Dexmedetomidine attenuates ischemia/reperfusion-induced myocardial inflammation and apoptosis through inhibiting endoplasmic reticulum stress signaling. J Inflamm Res. 2021; 14: 1217–1233. [Medline] [CrossRef]
39. Ghaderi S, Alidadiani N, Dilaver N, Heidari HR, Parvizi R, Rahbarghazi R, et al. Role of glycogen synthase kinase following myocardial infarction and ischemia-reperfusion. Apoptosis. 2017; 22: 887–897. [Medline] [CrossRef]
40. Dumont EA, Hofstra L, van Heerde WL, van den Eijnde S, Doevendans PA, DeMuinck E, et al. Cardiomyocyte death induced by myocardial ischemia and reperfusion: measurement with recombinant human annexin-V in a mouse model. Circulation. 2000; 102: 1564–1568. [Medline] [CrossRef]
41. Cai Z, Deng X, Jia J, Wang D, Yuan G. Ectodysplasin A/Ectodysplasin A receptor system and their roles in multiple diseases. Front Physiol. 2021; 12: 788411. [Medline] [CrossRef]
42. Sisto M, Lorusso L, Lisi S. X-linked ectodermal dysplasia receptor (XEDAR) gene silencing prevents caspase-3-mediated apoptosis in Sjögren's syndrome. Clin Exp Med. 2017; 17: 111–119. [Medline] [CrossRef]
43. Chang B, Punj V, Shindo M, Chaudhary PM. Adenoviral-mediated gene transfer of ectodysplasin-A2 results in induction of apoptosis and cell-cycle arrest in osteosarcoma cell lines. Cancer Gene Ther. 2007; 14: 927–933. [Medline] [CrossRef]
44. Wu Y, Leng Y, Meng Q, Xue R, Zhao B, Zhan L, et al. Suppression of excessive histone deacetylases activity in diabetic hearts attenuates myocardial ischemia/reperfusion injury via mitochondria apoptosis pathway. J Diabetes Res. 2017; 2017: 8208065. [Medline] [CrossRef]
45. Chimenti MS, Sunzini F, Fiorucci L, Botti E, Fonti GL, Conigliaro P, et al. Potential role of cytochrome c and tryptase in psoriasis and psoriatic arthritis pathogenesis: focus on resistance to apoptosis and oxidative stress. Front Immunol. 2018; 9: 2363. [Medline] [CrossRef]
46. Crow MT, Mani K, Nam YJ, Kitsis RN. The mitochondrial death pathway and cardiac myocyte apoptosis. Circ Res. 2004; 95: 957–970. [Medline] [CrossRef]
47. Wang X, Lu X, Zhu R, Zhang K, Li S, Chen Z, et al. Betulinic acid induces apoptosis in differentiated PC12 cells via ROS-mediated mitochondrial pathway. Neurochem Res. 2017; 42: 1130–1140. [Medline] [CrossRef]
48. Yilmaz MI, Romano M, Basarali MK, Elzagallaai A, Karaman M, Demir Z, et al. The Effect of Corrected Inflammation, Oxidative Stress and Endothelial Dysfunction on Fmd levels in patients with selected chronic diseases: a quasi-experimental study. Sci Rep. 2020; 10: 9018. [Medline] [CrossRef]
49. Kalogeris T, Bao Y, Korthuis RJ. Mitochondrial reactive oxygen species: a double edged sword in ischemia/reperfusion vs preconditioning. Redox Biol. 2014; 2: 702–714. [Medline] [CrossRef]
50. Kong L, Li W, Chang E, Wang W, Shen N, Xu X, et al. mtDNA-STING axis mediates microglial polarization via IRF3/NF-kappaB signaling after ischemic stroke. Front Immunol. 2022; 13: 860977. [Medline] [CrossRef]
51. Driessler F, Venstrom K, Sabat R, Asadullah K, Schottelius AJ. Molecular mechanisms of interleukin-10-mediated inhibition of NF-kappaB activity: a role for p50. Clin Exp Immunol. 2004; 135: 64–73. [Medline] [CrossRef]
52. Song L, Chang R, Sun X, Lu L, Gao H, Lu H, et al. Macrophage-derived EDA-A2 inhibits intestinal stem cells by targeting miR-494/EDA2R/β-catenin signaling in mice. Commun Biol. 2021; 4: 213. [Medline] [CrossRef]
53. Verhelst K, Gardam S, Borghi A, Kreike M, Carpentier I, Beyaert R. XEDAR activates the non-canonical NF-κB pathway. Biochem Biophys Res Commun. 2015; 465: 275–280. [Medline] [CrossRef]